IMAGING ELECTRICAL RESISTIVITY IN A SIMULATED LIMB BY MAGNETIC INDUCTION TOMOGRAPHY

S Watson*, R J Williams* and H Griffiths**

* School of Electronics, University of Glamorgan, Pontypridd, CF37 1DL, UK
** Dept. of Medical Physics & Clinical Engineering, Singleton Hospital, Swansea SA2 8QA, UK

Swatson1@glam.ac.uk

Abstract: Magnetic induction tomography (MIT) is a non-contact technique for imaging the electrical resistivity of biological tissues which may be applicable to the detection of lymphoedema in limbs. In this study a limb was modelled as a cylinder of diameter 10cm, length 20cm and homogeneous conductivity 1 Sm^{-1}. A finite difference model was used to compute the sensitivity distribution within the limb for three coil array geometries. For two geometries, the resulting sensitivity distributions were biased towards the periphery of the object with little sensitivity near the centre. Changing the dimensions of the coils and scanning them past the object produced no improvement in central sensitivity. The third geometry, however, involving a coil encircling the limb, produced an improved sensitivity near the centre but poorer longitudinal localisation.

Introduction

Magnetic induction tomography (MIT) is a non-contact technique for imaging the electrical resistivity of biological tissues. Coils induce eddy currents within the tissue and detect the resulting magnetic field perturbations the eddy currents produce, allowing the resistivity of the tissues to be determined [1]. The technique may be applicable to the detection of oedema, such as lymphoedema in limbs. A contactless MIT system could allow fast measurement and imaging of tissue fluid status and distribution along a limb and should be relatively easy to apply in a clinical setting in comparison to, for example, an EIT imaging system requiring electrodes to be attached.

The ability of a MIT system accurately to measure and image resistivity distributions within a conductive object is directly related to the system's sensitivity to resistivity changes throughout the object's volume. Low-frequency magnetic fields easily penetrate into biological tissues and for this reason it may be thought that high sensitivity within central volumes should be achievable. An MIT system's sensitivity distribution depends however on the eddy current distribution within the object. Scharfetter *et al* [2] computed the sensitivity maps for low-contrast perturbations in a conducting background and found that, for the coil geometry they employed, the maximum sensitivity lay on the periphery of the object and that the sensitivity maps were strongly dependent on both the conductivity contrast and the shape of the object.

The aim of this study was to assess the MIT sensitivity distributions likely to be obtained within human limbs. The distributions within a simple limb model were computed for three coil geometries. Coil parameters in the model such as dimensions and position were then varied to determine the factors which strongly influenced the sensitivity distributions.

Materials and Methods

A limb was modelled as a cylinder of diameter 10cm, length 20cm and homogeneous conductivity 1 Sm^{-1}. The quasi-static finite-difference algorithm described in [3] was employed to calculate the eddy-current distribution produced within the limb by each coil configuration. The sensitivity maps within the limb were computed using the reciprocity theorem [4], with the 'lead fields' in this case being the eddy current densities produced by the excitation coils J_{Ei} and detection coils J_{Di}. For a given pair of coils, the sensitivity is independent of which coil is used as the excitor and which is used as the detector. For each excitation/detection coil combination, the sensitivity S_i of voxel i with conductivity σ_i is given by

$$S_i = \frac{\overline{J_{Ei}}.\overline{J_{Di}}}{\sigma_i}$$

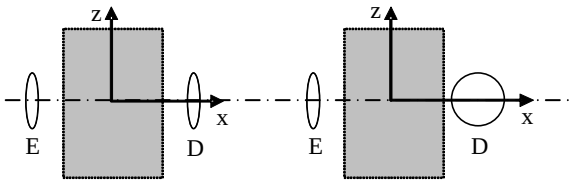

(a) (b)

Figure 1. Illustration of the first two coil geometries simulated. The limb's axis lies along Oz and its cross-section is shown in grey. E=excitation coil, D=Detector coil

ISSN: 1727-1983

The first two coil geometries employed are shown in Figure 1. In Figure 1(a) both coils' axes are oriented in the x-direction with the excitation coil at position (-12.5, 0, 0) (units in cm) and the detector coil at (12.5, 0, 0). In Figure 1(b) the coils are positioned as in the first case but coil D is oriented such that its axis points in the y-direction (normal to page) to minimise coupling with the primary field, thereby greatly improving the system's SNR; this has been termed the 'right-angle' or 'zero-flux' method [5, 6] . All the coils were 5 cm in diameter.

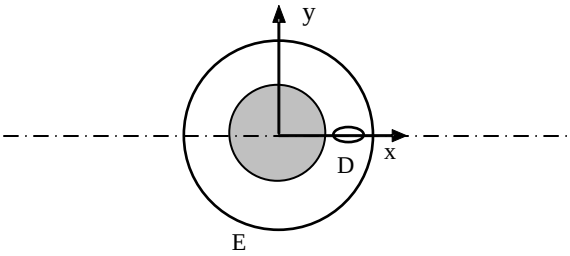

Figure 2. Illustration of the 'encircling' excitation coil geometry simulated.

Lastly, a very different coil geometry was modelled employing large excitation coil encircling the limb (figure 2). The excitation coil, of diameter 20cm, was placed at position (0, 0, 0) and oriented with its axis in the z-direction. A small detector coil, of diameter 1 cm, was placed at (7.5, 0, 0) and oriented with its axis in the y-direction, again as a 'zero-flux' configuration

Results

The normalised sensitivity maps produced by the first two geometries (Figures 1a and 1b) are shown in Figure 3 for six cross-sections of the simulated limb, z = 0, 2, 4, 6, 8 and 10.

For both coil geometries, the maximum sensitivity lay at the periphery of the object on the cross-sections z=0 to 6 and was observed to be very low near the centre of the object. The area of slightly higher sensitivity observed near the centre of the cross-section at z=10cm for coil geometry (a) is believed to be a boundary effect, the eddy currents being 'compressed' at the ends of the cylinder.

To test the effect of coil diameter on the sensitivity distributions, the diameters of the excitation and detection coils were changed to four different pairs of values (in cm): 1 and 5, 5 and 1, 1 and 1, 15 and 15. The sensitivity maps were again computed. In each case it was found that although the magnitude of the sensitivity varied with the coil dimensions, the spatial distribution of the normalised sensitivity did not change; hence the coil diameter was not found to be important.

With the diameters of both coils set again at 5 cm, the coil pair was now scanned in the y-direction in 2 cm steps from y=0, to y=4 as shown in Figure 4. The resulting sensitivity maps produced for each position are shown in Figure 5 for the cross-section z=0.

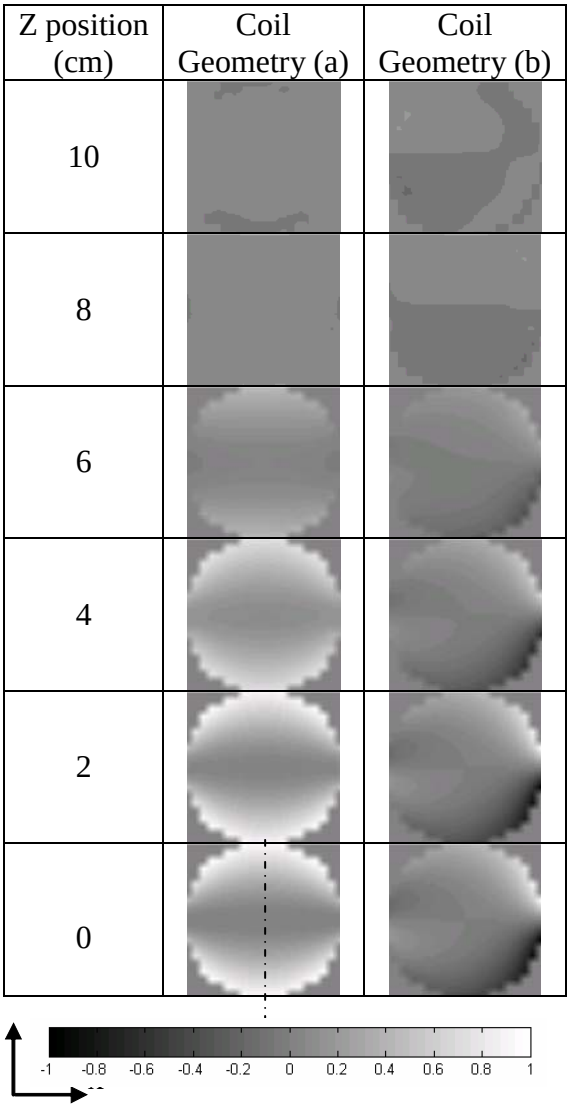

Figure 3. Sensitivity distributions at cross-sections z=0, 2, 4, 8 and 10. The second and third columns represent the distributions for the coil geometries of figure 1(a) and 1(b) respectively. The dashed line shows the profile used for the sensitivity plot in figure 7.

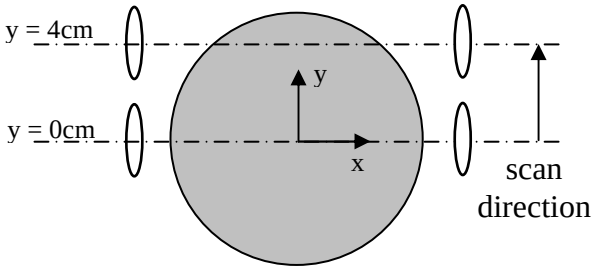

Figure 4. Scanning the coils towards the edge of the simulated limb.

ISSN: 1727-1983

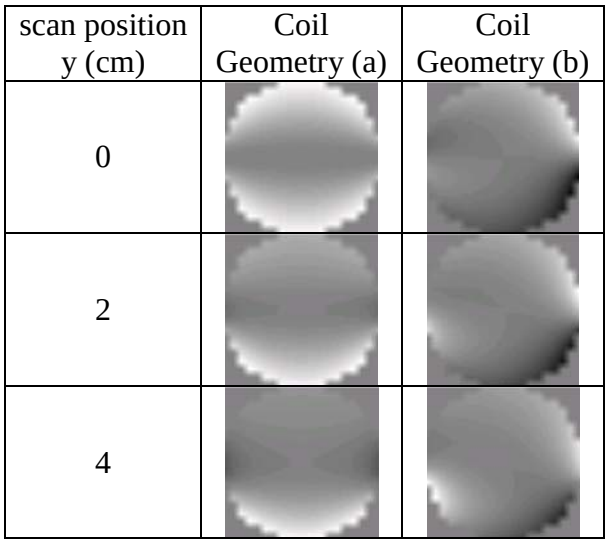

Figure 5. Sensitivity distributions at cross-section z = 0 for the scan positions y = 0, 2 and 4. The second and third columns represent the distributions for the coil geometries of figure 1(a) and 1(b) respectively.

Scanning the coils in the y-direction did not appear to result in an increase in the sensitivity within the central volume of the limb. The area of maximum sensitivity again appeared on the periphery in each case and the outcome of scanning the coil pair was simply to increase the sensitivity on one side of the volume relative to the other side.

For the third coil geometry, with the encircling excitation coil (figure 2), the sensitivity maps are displayed in figure 6. Although the sensitivity at the exact centre is still zero, a significantly higher sensitivity is produced nearby. In fact, the distribution is anti-symmetrical about the plane y=0, giving a large gradient of sensitivity at the centre. However, the improvement in the sensitivity in the region of the centre appears to be at the cost of a decrease in its localisation in the z-direction, the highest sensitivity being located at z=6, i.e. 6 cm out of the plane of the excitation coil.

Figure 7 shows a profile taken across the cross-section z=6 for this coil geometry and for comparison, the profile produced by the coil geometry shown in figure 1(a) (see also dashed line in figure 3), showing how very different the two are.

Discussion

For two of the MIT coil geometries simulated, the sensitivity within a simulated limb was found to be distributed towards the periphery with little or no sensitivity at the centre. Varying the coil dimensions or displacing the coils to one side of the object (figure 4) were found to produce no benefit as regards increasing the central sensitivity. The shape of the limb itself was the dominant factor in determining the sensitivity distribution. The fall-off in sensitivity with depth for the

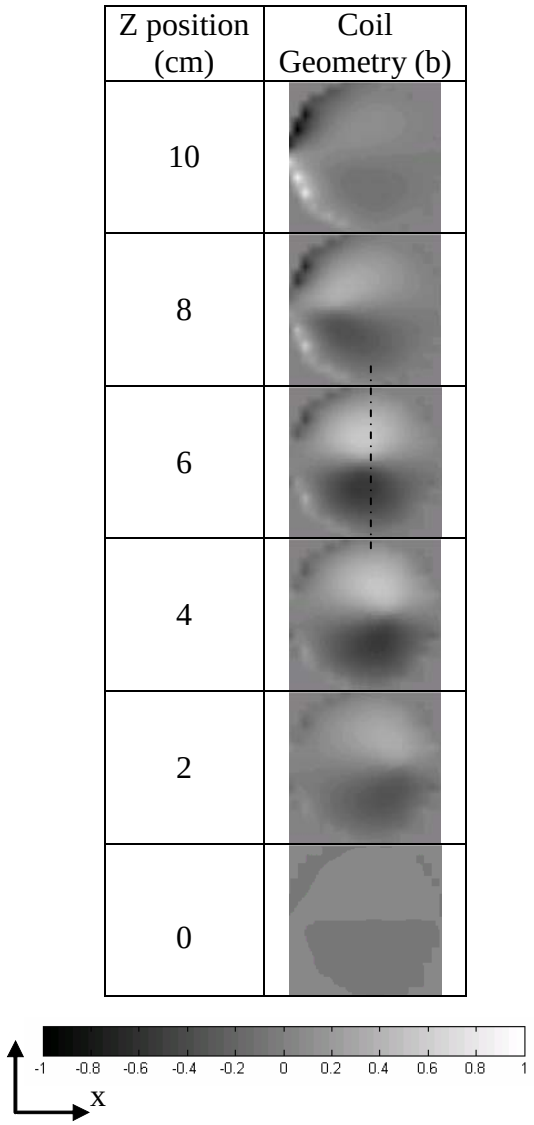

Figure 6. Sensitivity distributions at cross-sections z=0, 2, 4, 8 and 10. The dashed line shows the profile used for the sensitivity plot in figure 7.

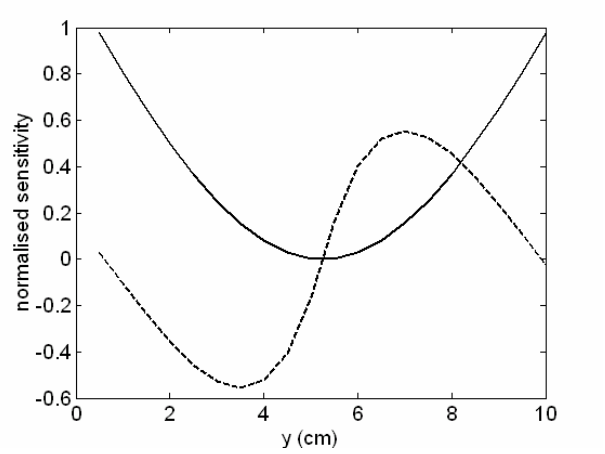

Figure 7. Senstivity profiles for the geometry shown in figure 1(a) (solid line) and that shown in figure 2 (dashed line).

ISSN: 1727-1983

coil geometry of figure 1(a), shown in figure 7, was such that 50% of the received signal would be derived from tissues within 1 cm of the surface and 90% from within 2.5 cm.

The non-contact nature of MIT makes it attractive for a range of biomedical applications such as detection of oedema within limbs, torso and brain [7] and in body composition studies [8]. The conventional MIT coil geometries used in this study involving small coils at the periphery of the object, appear to have very limited sensitivity at depth. The received signal will be predominantly produced in human limbs by tissues of high conductivity, such as blood or muscle, within the first few centimetres of the skin surface. It is possible, though, that even with the sensitivity confined to the superficial layers, an MIT system could be used for monitoring regional oedema in the limb as the superficial tissues are affected.

Preliminary investigations of a coil configuration using a large coil encircling the limb suggest that higher sensitivity within the central volume may be achievable. This is similar in concept to the work of Freeston and Tozer [9] and others who have used encircling coils for inducing eddy currents, but electrodes attached to the object for detecting the signals. In the present study, there are no electrodes, the system being entirely inductive and contactless. Further work in developing this configuration into a full MIT array will be the next step in our research.

References

[1] GRIFFITHS H (2005) Magnetic Induction Tomography. In *Electrical Impedance Tomography: Methods, History and Applications* (ed. D.S. Holder), pp213-38. Institute of Physics Publishing, UK. ISBN 0 7503 0952 0

[2] SCHARFETTER, H., RIU, P., POPULO, M. & ROSELL, J. (2002) Sensitivity maps for low-contrast perturbations within conducting background in magnetic induction tomography, *Physiological Measurement*, 23, 195-202.

[3] MORRIS, A., GRIFFITHS, H. & GOUGH, W. (2001) A numerical model for magnetic induction tomographic measurements in biological tissues, *Physiological Measurement*, 22, 113-119.

[4] GESELOWITZ, D. (1971) An application of electrocardiographic lead theory to impedance plethysmography, *IEEE Transactions on Biomedical Engineering*, 18, 38-41.

[5] WATSON, S., MORRIS, A., WILLIAMS, R. J., GRIFFITHS, H. & GOUGH, W. (2004) A primary field compensation scheme for planar array magnetic induction tomography, *Physiological Measurement*, 25, 271-279.

[6] SCHARFETTER, H. & PILZ, K. (2005) A new type of gradiometer for the receiving circuit of magnetic induction tomography, *Physiological Measurement*, 26, S307-317.

[7] MERWA, R., HOLLAUS, K., OSZKAR, B. & SCHARFETTER, H. (2004) Detection of brain oedema using magnetic induction tomography: a feasibility study of the likely sensitivity and detectability, *Physiological Measurement*, 25, 347-354.

[8] PEYTON A., TAPP H.S., KTISTIS C. et al. (2004) The development of a novel body scanner to measure human composition, Paper presented at the *XII International Conference on Electrical Bio-Impedance*, Manchester, UK.

[9] FREESTON I.L., TOZER R.C. (1995) Impedance imaging using induced currents. *Phys. Meas.* 16 Suppl. 3A 257-66

ISSN: 1727-1983